

Response Surface Optimization of Process Conditions and Characteristics of Nanostarch-based Biocomposite Film Reinforced by Cellulose Nanocrystals

Qijie Chen,* Liling Zhou, Jiaqi Zou, and Jianhui Wang

Nanostarch has attracted much research interest recently due to its biodegradability and biocompatibility. A type of biocomposite film based on corn nanostarch (CNS) as the matrix and cellulose nanocrystals (CNC) as the reinforcement was prepared using a solution casting method. The influences of corn nanostarch concentration (C_{CNS}), glycerin dosage (D_g), and cellulose nanocrystals dosage (D_{CNC}) on the tensile strength of the biocomposite film were investigated by central composite design. The results were examined by an analysis of variance (ANOVA) and response surface methodology (RSM). The optimized process conditions as follows: C_{CNS} of 11.25%, D_g of 12.00%, and D_{CNC} of 5.00%. The CNS/CNC biocomposite film produced under these conditions showed a high tensile strength of 12.90 MPa. The CNS/CNC biocomposite film was characterized by Fourier transform infrared spectroscopy (FTIR), differential scanning calorimetry (DSC), water contact angle, and scanning electron microscopy (SEM). The CNS/CNC biocomposite film has potential application prospects in the field of food and biomedical packaging.

Keywords: Corn nanostarch; Cellulose nanocrystals; Biocomposite film; Response surface methodology

Contact information: Hunan Provincial Engineering Research Center for Food Processing of Aquatic Biotic Resources, School of Chemistry and Food Engineering, Changsha University of Science and Technology, Changsha, Hunan Province, 410114, People's Republic of China;

* Corresponding author: chenqijie@126.com (Qijie Chen)

INTRODUCTION

Biocomposite film has received attention in the packaging of renewable sources due to the consumption of fossil fuel and environmental pollution caused by traditional petroleum-based plastic food packaging. Starch is a renewable, inexpensive, and biodegradable natural material that is widely used in the food industry. Starch is composed of two glycosidic macromolecules containing amylose and amylopectin. Amylose is a linear polysaccharide composed of (1-4) α -D-glucopyranose with molecular weight of 2×10^4 to 2×10^6 Daltons, and amylopectin is a high-branched macromolecule composed of both (1-4) and (1-6) α -D-glucopyranosyl linkages with molecular weight of 2×10^7 to 2×10^9 Daltons (Teixeira *et al.* 2014). Nanostarch is a research hotspot in the fields of biocomposites materials, food packaging, medicine, and cosmetics due to its advantages of small particle size, large specific surface area, high crystallinity, and biodegradability (Kim *et al.* 2015). Nanostarch can be prepared by various methods, including hydrolysis or enzymolysis, physical disintegration, twin screw extrusion, and self-assembly (Jiang *et al.* 2016; Chen *et al.* 2018).

Starch film has good barrier properties against oxygen, carbon dioxide, and lipids. Compared with traditional film made of synthetic polymers, starch films have poor tensile strength, which limits their industrial applications. However, much literature has shown that nanofillers can improve the mechanical properties of starch-based films, such as nanoclays (Müller *et al.* 2011), cellulose nanocrystals (CNC) or cellulose nanofiber (Pelissari *et al.* 2017), starch nanocrystals or nanoparticles (Li *et al.* 2015), and carbon nanotubes (Cheng *et al.* 2013).

Cellulose nanocrystal (CNC) is a rich natural biological polysaccharide with an ordered cellulose crystalline region, large specific surface area, and high surface energy, which make it an ideal material for biocomposite films. CNC has abundant -OH side groups, and it is easy to polymerize to achieve different mechanical properties. It can be used as reinforcement in various polymer matrices such as chitosan (Corsello *et al.* 2017), polylactide (Gazzotti *et al.* 2017), gum (Ma *et al.* 2017), polyvinyl alcohol (Singh *et al.* 2017), polyurethane (Santamaria-Echart *et al.* 2016), carboxymethyl cellulose (Li *et al.* 2016), poly(vinyl pyrrolidone) (Huang *et al.* 2016), and starch (Cui *et al.* 2017).

In this work, the corn nanostarch (CNS) was prepared by twin-screw extrusion, and it had better film forming properties than native starch (Chen *et al.* 2018). The biocomposite film based on corn nanostarch (CNS) as the matrix and cellulose nanocrystals (CNC) as the reinforcement was prepared using a solution casting method. And the optimal formulation of CNS/CNC biocomposite film was investigated by response surface methodology (RSM) and analysis of variance (ANOVA). The optimized CNS/CNC biocomposite films were also characterized by Fourier transform infrared spectroscopy (FTIR), differential scanning calorimetry (DSC), water contact angle, and scanning electron microscope (SEM).

EXPERIMENTAL

Raw Materials

Corn nanostarch (CNS) was prepared by extrusion in the laboratory according to the method described previously (Chen *et al.* 2018). The preparation process was as follows: corn starch was premixed with 10.0% glycerin and then mixed in a high-speed homogenizer. The mixture was fed into twin-screw extruder with twelve barrels, and the crosslinking agent of 2.0% glyoxal was injected to the extruder from the tenth barrel. The extrudate was dried and smashed to obtain the corn nanostarch. Bleached sulfate softwood pulp was provided from Yueyang paper Co. Ltd. (Hunan province, China). Glycerol, sulfuric acid, and sodium hydroxide were supplied by Sinopharm Chemical Reagents Co., Ltd (Shanghai, China). All other reagents were commercially available and of analytical grade.

Preparation of Cellulose Nanocrystals (CNC)

CNC was extracted from bleached sulfate softwood pulp as previously described (Yu *et al.* 2017). A total of 10.00 g of bleached sulfate softwood pulp was hydrolyzed in 80 mL of H₂SO₄ (64% mass concentration) at 45 °C for 2 h with continuously stirring, followed by successive centrifugation for 10 min at 4000 rpm until neutralization, and dialysis in distilled water.

Preparation of CNS/CNC Biocomposite Film

Different proportions of CNS, glycerol, and CNC biocomposite film was prepared by casting. First, CNS was added to the distilled water to form slurry, followed by stirring at 70 °C for 30 min. Glycerol (based on the dry CNS) was added as a plasticizer and stirred at 70 °C for another 20 min. Finally the CNC (based on the dry CNS) was added to the mixed solution, and the solution was treated with an ultrasonic wave (VOSHIN-501D, Voshin Instruments Manufacture Co., Ltd, Wuxi, China) at 120 W for 30 min to ensure uniform suspension. After vacuum degassing to remove air bubbles, the mixed solution was placed on Petri dishes and dried at 45 °C at a relative humidity (RH) of 45% for 72 h in desiccators containing a saturated NaBr solution. The thickness of film was about 0.3 mm.

The values of corn nanostarch concentration (C_{CNS}), glycerol dosage (D_{g}), and cellulose nanocrystals dosage (D_{CNC}) were varied according to three variables-three levels of a Central Composite Design (CCD) as reported in Table 1. Preliminary tests were performed under process conditions at the CCD central point to determine the ideal moisture content of the films. For this purpose, a film sample was weighed every 10 min, until the film could be easily removed from the Petri dish without any damage.

Tensile Strength

Biocomposite film samples were stored at 45% RH for 72 h before the tensile strength was determined using a tensile testing machine (DCP-KZW300, Sichuan Changjiang Papermaking Instruments Co., Ltd, Yibin, China) according to the ASTM D882-02 (2002) standard. The tensile strength (TS/MPa) was calculated with Eq. 1,

$$TS = \frac{F}{A} \quad (1)$$

where F is the required maximum load (N), stretching the biocomposite film to the breaking point, and A is the cross-sectional area (mm^2).

Transmission Electron Microscopy (TEM)

TEM observation of CNC were carried out by JEM-2100 transmission electron microscope (Tokyo, Japan). Ultrasonic treatment was performed on the diluted CNC suspension and a drop of CNC suspension was deposited on a glow-discharged carbon-coated copper grid of the TEM and dried at room temperature before the excess liquid was absorbed by filter paper. Uranyl acetate was deposited on the grid before the observation.

FTIR Spectral Analysis

FTIR spectra of pure CNS film and CNS/CNC biocomposite film were recorded by a Bruker Vertex 70v vacuum spectrometer (Karlsruhe, Germany) in reflection mode. The range was from 4000 cm^{-1} to 400 cm^{-1} , and the resolution was 2 cm^{-1} . The pellets were prepared from powder samples by the KBr method.

Differential Scanning Calorimetry

The DSC patterns of pure CNS film and CNS/CNC biocomposite film were examined on a TA Differential scanning calorimeter (Q2000, San Diego, CA, USA). The samples were sealed in an aluminum pan and heated from 0 to 200 °C at a rate of 10 °C/min.

Water Contact Angle

The water contact angle of pure CNS film and CNS/CNC biocomposite film was measured by the SDC 350 contact angle measuring instrument (Shanghai, China). The sample film was cut into a rectangular shape (10 mm × 50 mm). Deionized water was dropped on the film surface, and the contact angle was measured automatically.

Scanning Electron Microscopy

The samples were maintained in a desiccator with silica gel for 5 d before they were fractured in liquid nitrogen and sputter-coated with gold prior to examination. The surface morphology of the CNS and nanostarch-based biocomposite film was analyzed using a Jeol scanning electron microscope (JSM-6490LV, Kyoto, Japan) at an accelerating voltage of 10 to 15 kV.

Experimental Design and Statistical Analysis

The surface response methodology was used to study the effects of corn nanostarch concentration (C_{CNS}), glycerol dosage (D_g), and cellulose nanocrystals dosage (D_{CNC}) on the tensile strength of biocomposite film. It was defined according to a 2^3 full-factorial central composite design. An analysis of variance (ANOVA), RSM, and all statistical analyses were performed by Design-Expert 8.0.6.1 software (Stat-Ease, Minneapolis, MN, USA). ANOVA was used to evaluate the statistical significance of the developed quadratic mathematical model, including P value, F value, degrees of freedom (df), sum of squares (SS), coefficient of variation (CV), coefficient of determination (R^2), adjusted coefficient of determination (R^2_{Adj}), and predicted coefficient of determination (R^2_{Pred}). After fitting the data with the model, the response surface graph was constructed to predict the relationship between independent and dependent variables. The normal distribution of residuals, residuals and prediction equations, the actual and predicted values of the equations were analyzed, and the model fitted to the experimental data were measured. The polynomial of the fitting model was given in Eq. (2),

$$Y = \beta_0 + \sum_{i=1}^K \beta_i X_i + \sum_{i=1}^{K-1} \sum_{j=1}^K \beta_{ij} X_i X_j + \sum_{i=1}^K \beta_{ii} X_i^2 + e_i \quad (2)$$

where Y is the response (tensile strength); X_i are the coded of the independent variables (X_1, X_2, X_3); β_0, β_i , and β_{ij} are the model intercept coefficient, interaction coefficients of linear, quadratic and the second-order terms, respectively; K is the number of independent parameters; and e_i is the error.

RESULTS AND DISCUSSION

Mathematical Model and ANOVA

The results of 2^3 full-factorial central composite design are summarized in Table 1. The suitable ranges for the variables C_{CNS} , D_g , and D_{CNC} were determined on the basis of single-factor experiment. The value of Run 16 was equivalent to the variance analysis of D_{CNC} , which was used to analyze the experimental data and statistical significance of the established polynomial model. The P value is used to check whether the coefficients in the quadratic regression equation are significant ($P < 0.05$). The P value of multiple regression was very small ($\text{Prob} > F < 0.0001$), indicating that the model established could fully represent the real relationship among the selected parameters.

Table 1. Center Composite Design Matrix with Values of Factors and Responses to Tensile Strength of Biocomposite Film

Run	C _{CNS} (%)	D _g (%)	D _{CNC} (%)	TS (MPa)
2	10.00(0)	11.50(0)	3.50(0)	8.175
3	10.00(0)	8.98(-a)	3.50(0)	4.136
4	8.75(-1)	10.00(-1)	6.00(1)	6.816
5	8.75(-1)	10.00(-1)	1.00(-1)	5.527
6	8.75(-1)	13.00(1)	6.00(1)	5.699
7	7.90(-a)	11.50(0)	3.50(0)	7.891
8	10.00(0)	11.50(0)	3.50(0)	8.404
9	11.25(1)	10.00(-1)	1.00(-1)	4.847
10	11.25(1)	13.00(1)	6.00(1)	10.287
11	11.25(1)	13.00(1)	1.00(-1)	6.115
12	12.10(a)	11.50(0)	3.50(0)	10.145
13	10.00(0)	11.50(0)	3.50(0)	8.917
14	10.00(0)	11.50(0)	3.50(0)	8.219
15	10.00(0)	11.50(0)	7.70(a)	6.951
16	10.00(0)	11.50(0)	-0.70(-a)	3.546
17	10.00(0)	11.50(0)	3.50(0)	8.777
18	10.00(0)	11.50(0)	3.50(0)	8.598
19	11.25(1)	10.00(-1)	6.00(1)	7.208
20	8.75(-1)	13.00(1)	1.00(-1)	4.472

Table 2. ANOVA of the Quadratic Modulus of the Response Surface

Source	Sum of Squares	df	Mean Square	F Value	Prob > F
Model	75.66	9	8.41	67.25	< 0.0001
X ₁ :C _{CNS} /%	6.94	1	6.94	55.50	< 0.0001
X ₂ :D _g /%	0.71	1	0.71	5.66	0.0387
X ₃ :D _{CNC} /%	15.99	1	15.99	127.88	< 0.0001
X ₁ X ₂	5.31	1	5.31	42.49	< 0.0001
X ₁ X ₃	2.02	1	2.02	16.14	0.0025
X ₂ X ₃	0.38	1	0.38	3.06	0.1109
X ₁ ²	0.81	1	0.81	6.51	0.0288
X ₂ ²	27.85	1	27.85	222.82	< 0.0001
X ₃ ²	17.28	1	17.28	138.24	< 0.0001
Lack of Fit	0.80	5	0.16	1.76	0.2747
Std. Dev.	0.35	R ²	0.9837	–	–
Mean	6.97	^a R ² _{Adj}	0.9691	–	–
C.V. %	5.07	^b R ² _{Pred}	0.9040	–	–
PRESS	7.39	Adeq Precision	27.15	–	–

^aR²_{Adj} = adjusted R², ^bR²_{Pred} = predicted R²

As shown in Table 2, the model was highly significant (Prob > F < 0.001), and the responses of process variables have obvious effects on the tensile strength of biocomposite films. According to ANOVA, the coefficients of X₁, X₂, X₃, X₁X₂, X₁X₃, X₁², X₂², and X₃² had statistical significance (P < 0.05), indicating that the established model was in good agreement with the real data. The P coefficients of X₁ and X₃ were very small (P < 0.0001), which indicates that the CNS and CNC had the greatest influences on the tensile strength of the biocomposite film. This is because CNC is a high crystalline nanoparticle, with good mechanical properties and high stiffness and elastic modulus. CNS and CNC have similar

chemical properties, and the strength of biocomposite film was improved by hydrogen bonding. The "Lack of Fit F-value" of 1.76 implies the Lack of Fit is not significant compared with the pure error, and 27.47% of the probability of such a large "Lack of Fit F-value" was caused by inevitable error. The final fitting model obtained according to the variables was shown in Eq. 3:

$$Y = -11.16 - 8.032X_1 + 9.81X_2 - 0.618X_3 + 0.435X_1X_2 + 0.161X_1X_3 + 0.058X_2X_3 + 0.152X_1^2 - 0.618X_2^2 - 0.175X_3^2 \quad (3)$$

The goodness of the model fitting was checked by measuring the coefficient of determination (R^2) and the adjusted coefficient of determination (R^2_{Adj}). In this model, R^2 was 0.9837, indicating that the regression model can well explain 98% of the change in tensile strength process, and R^2_{Adj} was 97%, indicating that the experimental value was in good agreement with the predicted value (Yetilmmezsoy *et al.* 2009; You *et al.* 2019).

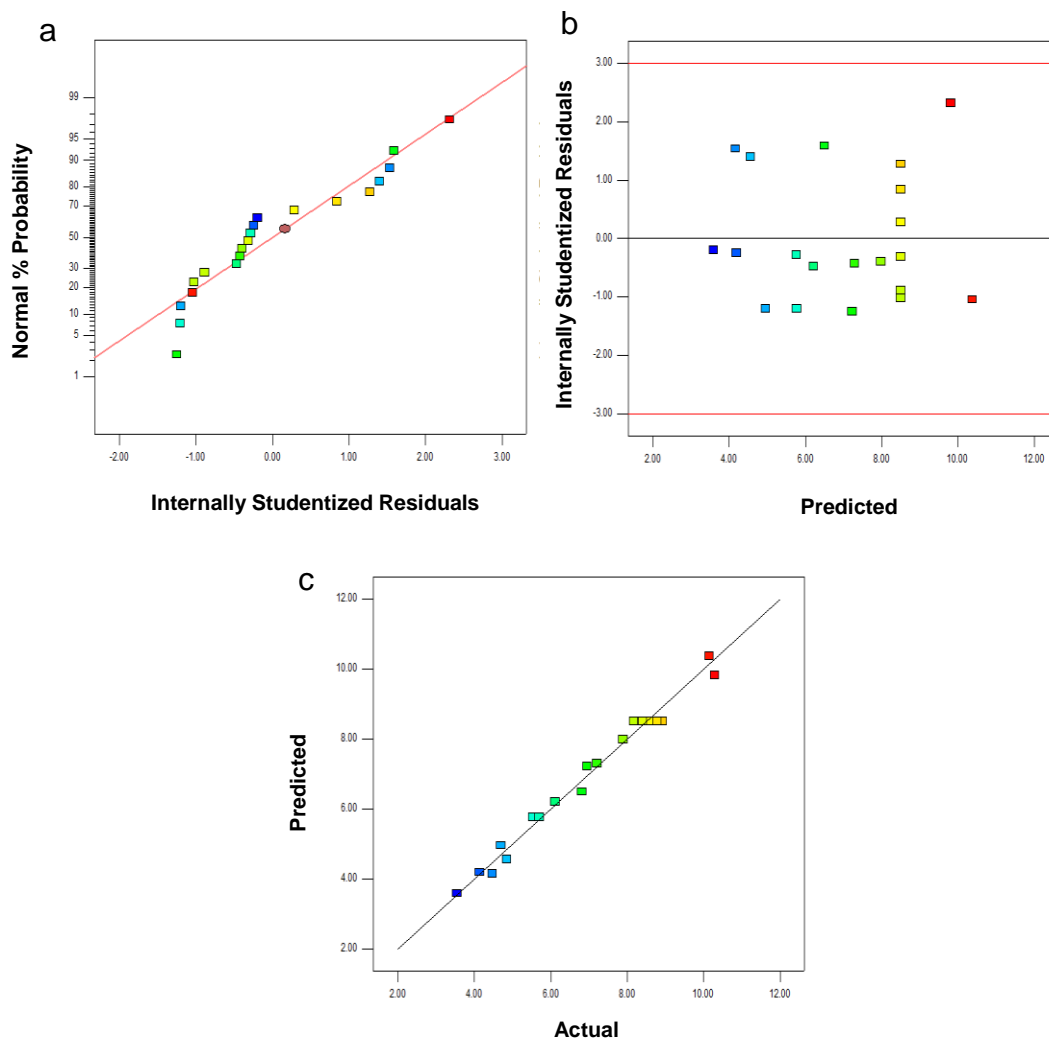


Fig. 1. Diagnostic plots of the quadratic model used for biocomposite film (a) Internally studentized residuals *versus* Normal percentage probability; (b) Predicted *versus* Internally studentized residuals; (c) Actual *versus* Predicted

Diagnosis of Model Adequacy

In general, exploration of fitted response surface models may yield poor or misleading results, unless the models show a good fit, which makes it critical to check the adequacy of the model. The normal distribution of the frequency graph of residuals is an intuitive test method, that is, the residuals fall within a certain range, and within the scope of the normal distribution with the corresponding probability distribution, indicating that the residuals obey the normal distribution. As shown in Fig. 1(a), the residuals and normal distributions of the experiment trial were concentrated in the range (2, 2), indicating that the model errors were normally distributed. According to the residual distribution diagram and the predicted values of the equation, the distribution of residual falling points and equations were discrete and irregular, indicating that the error of the model is small, as shown in Fig. 1(b). The corresponding relationship between the predicted graph and the measured value is shown in Fig. 1(c), the points in the graph are set on a straight line with the measured value, indicating a good correlation between predicted values and the measured values.

Interaction of Process Variables

On the basis of a quadratic ternary regression equation (Y), the three-dimensional response surface graph was drawn, which provided an intuitive view of the response system for understanding the interaction between different variables on the response. The three-dimensional response surface graph shows the top or bottom, and the highest point is the maximum value of the response surface.

While keeping one variable constant, the interactions of other variables on tensile strength were analyzed, as shown in Fig. 2. When the value of C_{CNS} was fixed, the tensile strength of the biocomposite film increased slightly as the glycerol dosage increased from 10.0% to 11.60%. However, many studies have shown that glycerol as a plasticizer reduces the intermolecular forces between polymers, thus enhancing the molecular fluidity and flexibility of the film (Mohsin *et al.* 2011). The opposite results were obtained, which may have no obvious effect on weakening intermolecular forces in the range of the dosage of glycerol. When the D_g was fixed at 10.0% to 11.60%, the increasing C_{CNS} enhanced the tensile strength of the biocomposite film. The total solid concentration of biocomposite film enhances the intermolecular forces by the formation of inter-molecular hydrogen bonds in the starch matrix. Figure 2(a) shows that the highest tensile strength resulted when lower D_g (12.05%) and high C_{CNS} (12.25%) were used.

Figure 2(b) shows that the 11.5% of D_g was selected as the center point and 8.75% of C_{CNS} was fixed. With the increase of D_{CNC} from 1.0% to 5.0%, the tensile strength of biocomposite film increased by 60%. Due to the geometric shape and stiffness of CNC, the reinforcement effect obtained by CNC is attributed to the formation of a rigid network formed by hydrogen bonds and the mutual entanglement of the CNS matrix. CNC has better mechanical properties than CNS, so it can be mixed with starch matrix to increase the tensile strength of the film. When D_{CNC} was increased from 5% to 6%, the tensile strength of the biocomposite film decreased slowly. This is due to the slight aggregation of CNC; the positive contribution of CNC to the tensile strength of the film decreased. Similarly, the interaction between C_{CNS} and D_{CNC} affected the tensile strength. When C_{CNS} was more than 10.25%, the D_{CNC} had a significant positive effect on the tensile strength of biocomposite film.

As shown in Fig. 2(c), when 11.25% of C_{CNS} was selected as the center point, the interaction between glycerol molecules and CNC had no obvious effect on the tensile

strength of the biocomposite film because the glycerol molecules only acted on the intermolecular and intramolecular hydrogen bonds in the starch matrix. The results showed that the C_{CNC} had greater influence on the tensile strength of biocomposite film more than D_g . The reduction of intermolecular force was not obvious in biocomposite films with lower D_g . However, the increase of D_g (12%) resulted in high mobility of the chains, and the intermolecular forces between adjacent CNC chains were weakened by glycerol molecules, which reduced the tensile strength of the biocomposite film.

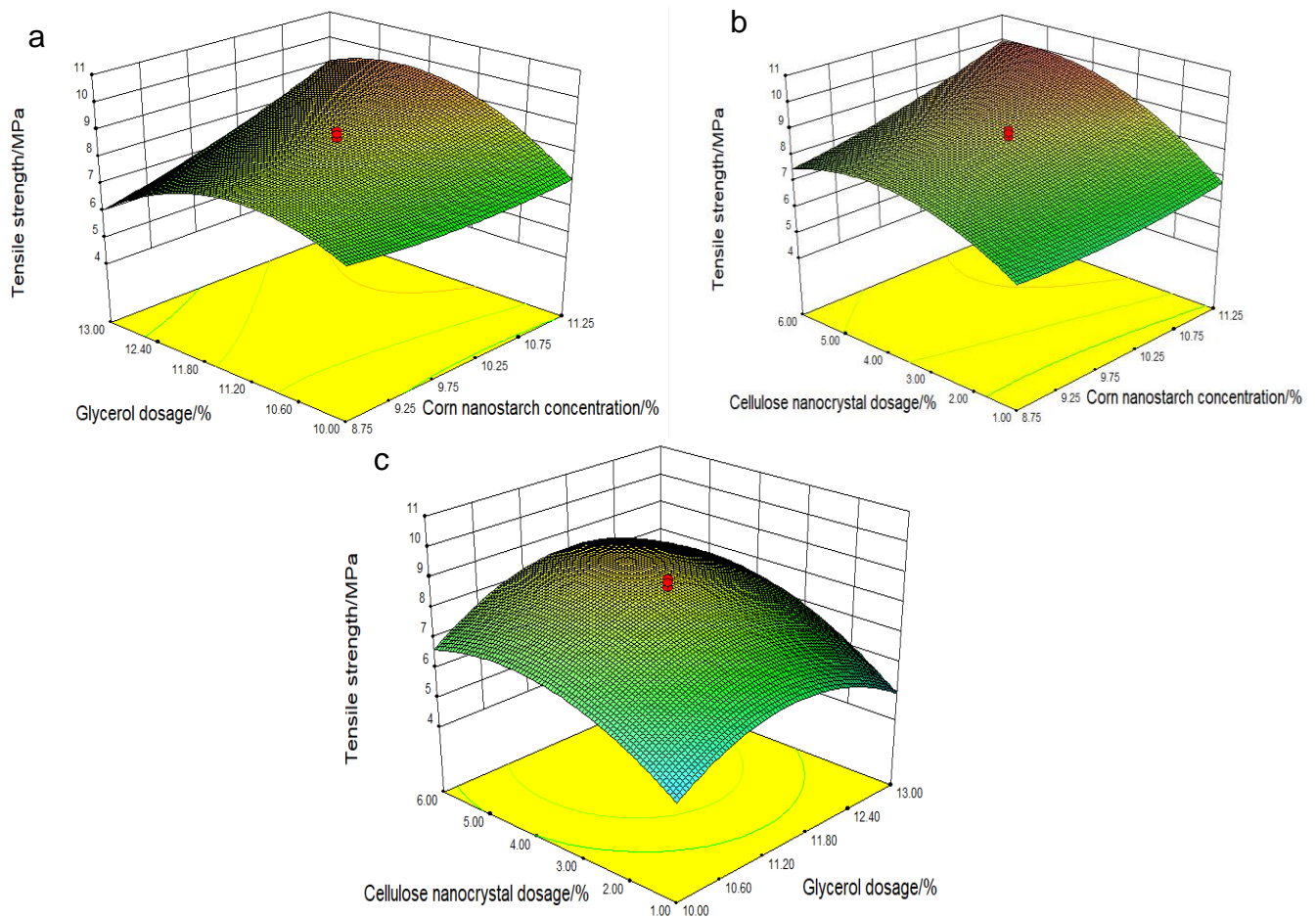


Fig. 2. Response surfaces for the tensile strength as a function of (a) corn nanostarch concentration (C_{CNS}) and glycerol dosage (D_g), (b) corn nanostarch concentration (C_{CNS}) and cellulose nanocrystal dosage (D_{CNC}), (c) glycerol dosage (D_g), and cellulose nanocrystal dosage (D_{CNC}).

In summary, the comparative analysis of response surface showed that CNC, interactive CNC, and CNS had positive effects on tensile strength of biocomposite films. CNC formed a stronger network structure by intra- and inter-molecular hydrogen bonds and the mutual entanglement of CNS matrix, which improved the tensile strength of CNS/CNC biocomposite films. By the analysis of each performance response surface, the optimized process conditions were defined to be C_{CNS} of 11.25%, D_g of 12.0%, and D_{CNC} of 5.0%. The CNS/CNC biocomposite film prepared under optimized process conditions showed the high tensile strength of 12.9 MPa.

Table 3 showed that the comparison of the tensile strength of various CNC-reinforced biocomposite film. The tensile strength of corn starch/CNC film (Miranda *et al.*

2015), banana starch/CNC film (Pelissari *et al.* 2017), and starch/CNC film (Ali *et al.* 2018) were reported as 6.8 MPa, 11.1 MPa, and 8.1 MPa, respectively. In the present study, the tensile strength of CNS/CNC film was 12.9 MPa. This showed that the CNS/CNC film had higher tensile strength than native starch/CNC film.

Table 3. Comparison of the Tensile Strength of Various CNC-reinforced Biocomposite Films

Biocomposite film	Corn starch/CNC film	Banana starch/CNC film	Starch/CNC film	Corn nanostarch/CNC film
Tensile Strength (MPa)	6.8	11.1	8.1	12.9
Reference	Miranda <i>et al.</i> (2015)	Pelissari <i>et al.</i> (2017)	Ali <i>et al.</i> (2018)	This work

TEM Analysis of CNC

The TEM of CNC are shown in Fig. 3. CNC has highly ordered crystallization because its amorphous zone was eliminated by acid hydrolysis. The CNC presented needle-like nanocrystals, with an average length (L) of 150 ± 50 nm, a diameter (D) of 30 ± 10 nm. The same result was reported by Martins *et al.* (2011). This confirmed that the suspension contained CNC, which was mainly composed of a single nanocrystal and some aggregates due to its high specific surface area.

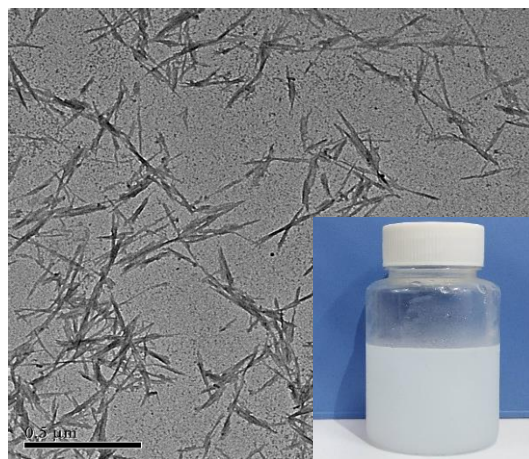


Fig. 3. TEM of CNC

FTIR Spectral Analysis of Biocomposite Film

The FTIR spectra of pure CNS film and optimized CNS/CNC biocomposite film are shown in Fig. 4. The peak at 3400 cm^{-1} corresponded to $-\text{OH}$ stretching vibration, and the peak at 2983 cm^{-1} was the symmetric vibration of $-\text{CH}_2$ groups. The bands located at 1630 cm^{-1} corresponded to the $-\text{OH}$ of bound molecular water (Cao *et al.* 2019). The peaks of CNS/CNC biocomposite film at 1440 cm^{-1} , 1087 cm^{-1} , 1043 cm^{-1} , and 879 cm^{-1} corresponded to $-\text{CH}_2$ scissoring motion, C-O stretching in the cellulose anhydrous glucose, and cellulosic β -glycosidic linkages, respectively (Sheng *et al.* 2018). These results confirmed that the CNS/CNC biocomposite film was uniformly mixed.

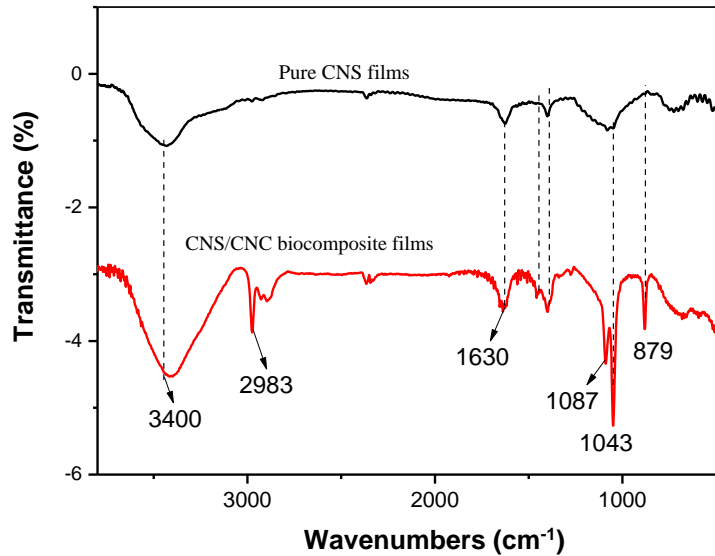


Fig. 4. FTIR spectra of pure CNS films and CNS/CNC biocomposite films

DSC Analysis of Biocomposite Film

The DSC thermograms of pure CNS film and optimized CNS/CNC biocomposite film are presented in Fig. 5. The DSC curves showed that the two kinds of films had similar degradation during the heating process, and the two curves had the similar broad absorption peak at 130 °C. The melting peak temperature of CNS/CNC biocomposite film increased slightly, which was mainly related to the high crystallinity of CNC, indicating that CNC had good dispersibility in the CNS matrix (Ma *et al.* 2017).

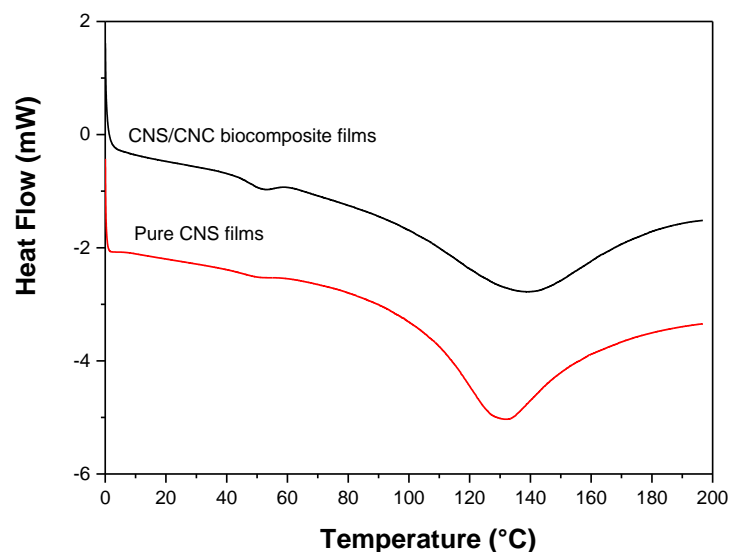


Fig. 5. DSC curves of pure CNS films and CNS /CNC biocomposite films

Water Contact Angle of Biocomposite Film

The water contact angle measurements of pure CNS film and CNS/CNC biocomposite film are shown in Fig. 6. A higher contact angle indicates a stronger hydrophobicity of the biocomposite film. The water contact angle of optimized CNS/CNC biocomposite film was 58.5° . The water contact angle of pure CNS film was 47.7° , and it was increased by 22.5%. The results showed that CNC improved the hydrophobicity of the biocomposite film, and the CNS/CNC biocomposite film had better water barrier property than the pure CNS film.

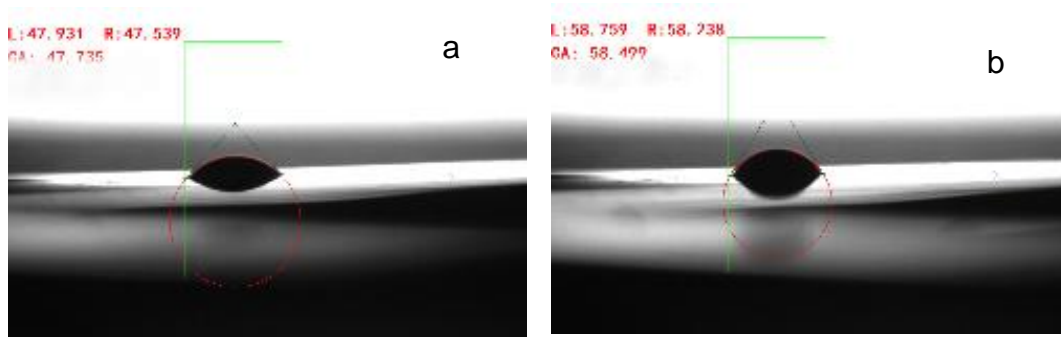


Fig. 6. Water contact angle of pure CNS film (a) and CNS/CNC biocomposite film (b)

SEM Analysis of Biocomposite Film

The SEM images of the CNS and CNS/CNC biocomposite film are presented in Fig. 7. Figure 7(a) shows that the CNS granules were complete and smooth, and their average particle size was about 100 nm. The surface of CNS/CNC biocomposite film was smooth without any deformation (Fig. 7(b)), indicating that CNC was evenly dispersed in the CNS matrix. As shown in Fig. 7(c), the CNC formed a stronger network structure by intra- and inter-molecular hydrogen bonds and mutual entanglement with CNS matrix. This also indicated that the addition of CNC greatly improved the tensile strength of CNS matrix film.

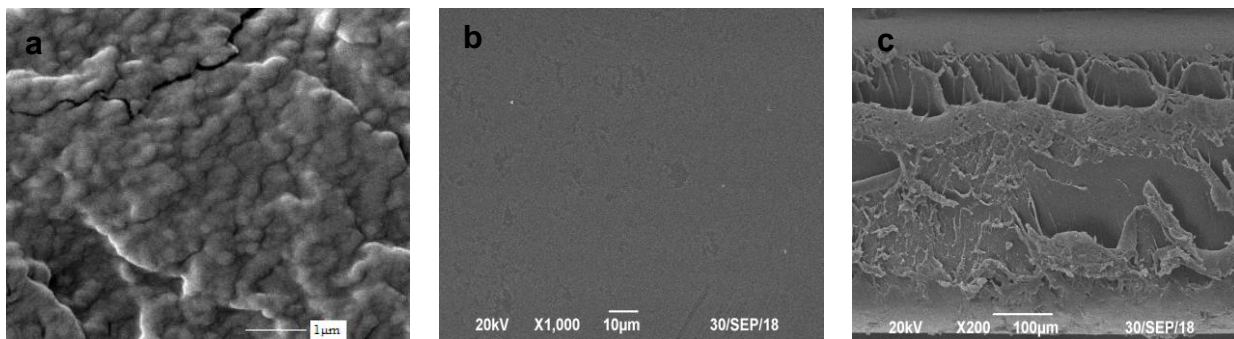


Fig. 7. SEM of CNS(a); the surface (b) and cross section (c) of CNS/CNC biocomposite film

CONCLUSIONS

1. An optimized process of nanostarch-based biocomposite film was successfully developed from corn nanostarch (CNS), glycerol, and cellulose nanocrystals (CNC) using the method of center composite design. The corn nanostarch concentration (C_{CNS}) and dosage of cellulose nanocrystals (D_{CNC}) had significant effects on the tensile strength of biocomposite film. By analysis of each performance response surface, the optimized process conditions were determined as C_{CNS} of 11.25%, a glycerine dosage (D_g) of 12.0%, and D_{CNC} of 5.0%, and the tensile strength of the optimized CNS/CNC biocomposite film was 12.9 MPa.
2. The CNC was homogeneously dispersed in CNS matrix in the CNS/CNC biocomposite film, and it increased the melting peak temperature slightly. The water contact angle of optimized CNS/CNC biocomposite film was increased by 22.5% and had better water barrier property than the pure CNS film. The CNS/ CNC biocomposite films have potential packaging applications in the field of food and biomedicine.

ACKNOWLEDGMENTS

This work was financially supported by the National Natural Science Foundation of China (No. 31500495), Hunan Provincial Education Department Foundation of China (No. 18B150) and Hunan Provincial Engineering Research Center for Food Processing of Aquatic Biotic Resources Foundation of China (No. 2018KJY03, 2018CT5010).

REFERENCES CITED

- Ali, A., Xie, F., Yu, L., Liu, H., Meng, L., Khalid, S., and Chen, L. (2018). "Preparation and characterization of starch-based composite films reinforced by polysaccharide-based crystals," *Composites Part B: Engineering* 133,122-128. DOI: 10.1016/j.compositesb.2017.09.017
- ASTM D882-02 (2002). "Standard test method for tensile properties of thin plastic sheeting," ASTM International, West Conshohocken, USA.
- Cao, Z., Li, W. F., Liu, C., Peng, Y. Y., Huang, Y., and Xiao, Z. L. (2019). "Development of potential embedded wireless sensor monitoring system based on low power bluetooth transmission," *Chinese J. Anal. Chem.* 47(2), 229-236. DOI: 10.19756/j.issn.0253-3820.181684
- Chen, Q., Dong, X., Zhou, L., Zheng, X., Wang, J., and Wang P. (2018). "Nanostarch surface coating of lightweight coated paper," *BioResources* 13(1), 729-739. DOI: 10.15376/biores.13.1.729-739
- Cheng, J., Zheng, P., Zhao, F., and Ma, X. (2013). "The composites based on plasticized starch and carbon nanotubes," *International Journal of Biological Macromolecules* 59(4), 13-19. DOI: 10.1016/j.ijbiomac.2013.04.010
- Corsello, F. A., Bolla, P. A., Anbinder, P. S., Serradell, M. A., Amalvy, J. I., and Peruzzo, P. J. (2017). "Morphology and properties of neutralized chitosan-cellulose nanocrystals nanocomposite films," *Carbohydrate Polymers* 156, 452-459. DOI: 10.1016/j.carbpol.2016.09.031

- Cui, S., Li, M., Zhang, S., Liu, J., Sun, Q., and Xiong, L. (2017). "Physicochemical properties of maize and sweet potato starches in the presence of cellulose nanocrystals," *Food Hydrocolloids* 77,220-227. DOI: 10.1016/j.foodhyd.2017.09.037
- Gazzotti, S., Farina, H., Lesma, G., Rampazzo, R., Piergiovanni, L., and Ortenzi, M. A. (2017). "Polylactide/cellulose nanocrystals: The *in situ* polymerization approach to improved nanocomposites," *European Polymer Journal* 94,173-184. DOI: 10.1016/j.eurpolymj.2017.07.014
- Huang, S., Zhou, L., Li, M.C., Wu, Q., Kojima, Y., and Zhou, D. (2016). "Preparation and properties of electrospun poly (vinyl pyrrolidone)/cellulose nanocrystal/silver nanoparticle composite fibers," *Materials* 9(7), 523-533. DOI:10.3390/ma9070523
- Jiang, S., Liu, C., Wang, X., Xiong, L., and Sun, Q. (2016). "Physicochemical properties of starch nanocomposite films enhanced by self-assembled potato starch nanoparticles," *LWT - Food Science and Technology* 69(2), 251-257. DOI: 10.1016/j.lwt.2016.01.053
- Kim, H. Y., Park, S. S., and Lim, S. T. (2015). "Preparation, characterization and utilization of starch nanoparticles," *Colloids & Surfaces B: Biointerfaces* 126, 607-620. DOI: 10.1016/j.colsurfb.2014.11.011
- Li, M.C., Mei, C., Xu, X., Lee, S., and Wu, Q. (2016). "Cationic surface modification of cellulose nanocrystals: Toward tailoring dispersion and interface in carboxymethyl cellulose films," *Polymer* 107, 200-210. DOI:10.1016/j.polymer.2016.11.022
- Li, X., Qiu, C., Ji, N., Sun, C., Xiong, L., and Sun, Q. (2015). "Mechanical, barrier and morphological properties of starch nanocrystals-reinforced pea starch films," *Carbohydrate Polymers* 121, 155-162. DOI:10.1016/j.carbpol.2014.12.040
- Ma, X., Cheng, Y., Qin, X., Guo, T., Deng, J., and Liu, X. (2017). "Hydrophilic modification of cellulose nanocrystals improves the physicochemical properties of cassava starch-based nanocomposite films," *LWT- Food Science and Technology* 86,318-326. DOI:10.1016/j.lwt.2017.08.012
- Martins, M. A., Teixeira, E. M., Corrêa, A.C., (2011). "Extraction and characterization of cellulose whiskers from commercial cotton fibers," *Journal of Materials Science* 46(24):7858-7864. DOI:10.1007/s10853-011-5767-2
- Miranda, C. S., Ferreira, M. S., Magalhães, M. T., Santos, W. J., Oliveira, J. C., Silva, J. B. A., and José, N. M. (2015). "Mechanical, thermal and barrier properties of starch-based films plasticized with glycerol and lignin and reinforced with cellulose nanocrystals," *Materials Today: Proceedings* 2(1), 63-69. DOI:10.1016/j.matpr.2015.04.009
- Mohsin, M., Hossin, A., and Haik, Y. (2011). "Thermal and mechanical properties of poly (vinyl alcohol) plasticized with glycerol," *Journal of Applied Polymer Science* 122(5), 3102-3109. DOI: 10.1002/app.34229
- Müller, C. M. O., Laurindo, J. B., and Yamashita, F. (2011). "Effect of nanoclay incorporation method on mechanical and water vapor barrier properties of starch-based films," *Industrial Crops and Products* 33(3), 605-610. DOI:10.1016/j.indcrop.2010.12.021
- Pelissari, F. M., Andrademahecha, M. M., Pjda, S., and Menegalli, F. C. (2017). "Nanocomposites based on banana starch reinforced with cellulose nanofibers isolated from banana peels," *Journal of Colloid & Interface Science* 505, 154-167. DOI: 10.1016/j.jcis.2017.05.106
- Santamaria-Echart, A., Ugarte, L., García-Astrain, C., Arbelaz, A., Corcuera, M. A., and Eceiza, A. (2016). "Cellulose nanocrystals reinforced environmentally-friendly

- waterborne polyurethane nanocomposites,” *Carbohydrate Polymers* 151, 1203-1209. DOI: 10.1016/j.carbpol.2016.06.069
- Sheng, Y. Y., You, Y., Cao, Z., Liu, L., and Wu, H. C. (2018). “Rapid and selective DNA-based detection of melamine using α -Hemolysin nanopore,” *Analyst* 143(10), 2411-2415. DOI: 10.1039/c8an00580j
- Singh, S., Gaikwad, K. K., and Lee, Y. S. (2017). “Antimicrobial and antioxidant properties of polyvinyl alcohol biocomposite films containing seaweed extracted cellulose nano-crystal and basil leaves extract,” *International Journal of Biological Macromolecules* 107 (Pt B), 1879-1887. DOI: 10.1016/j.ijbiomac.2017.10.057
- Teixeira, E. D., Decampos, A., Marconcini, J. M., Bondancia, T. J., Wood, D., and Klamczynski, A. (2014). “Starch/fiber/poly (lactic acid) foam and compressed foam composites,” *RSC Advances* 4(13), 6616-6623. DOI: 10.1039/c3ra47395c
- Yetilmezsoy, K., Demirel, S., and Vanderbei, R. J. (2009). “Response surface modeling of Pb (II) removal from aqueous solution by *Pistacia vera* L.: Box–Behnken experimental design,” *Journal of Hazardous Materials* 171(1-3), 551-562. DOI: 10.1016/j.jhazmat.2009.06.035
- You, Y., Zhou, K., Guo, B. Y., Liu, Q. S., Cao, Z., Liu, L., and Wu, H. C. (2019). “Measuring binding constants of cucurbituril-based host-guest interactions at the single-molecule level with nanopores,” *ACS Sensors* 4, 774-779. DOI: 10.1021/acssensors.9b00408
- Yu, Z., Alsammarraie, F. K., Nayigiziki, F. X., Wang, W., Vardhanabhuti, B., and Mustapha, A. (2017). “Effect and mechanism of cellulose nanofibrils on the active functions of biopolymer-based nanocomposite films,” *Food Research International* 99(Pt 1), 166-172. DOI: 10.1016/j.foodres.2017.05.009

Article submitted: February 9, 2019; Peer review completed: March 27, 2019; Revised version received and accepted: April 6, 2019; Published: April 16, 2019.
DOI: 10.15376/biores.14.2.4344-4357